Homogeneous and inhomogeneous linewidths of Eu^{3+} in disordered crystalline systems

K. W. Jang and R. S. Meltzer
Department of Physics and Astronomy, University of Georgia, Athens, Georgia 30602
(Received 27 March 1995)

The role of disorder on the inhomogeneous and homogeneous linewidths of Eu^{3+} in single crystals with various degrees of disorder is described for samples grown by LHPG (laser-heated pedestal growth). Emission spectra, hole-burning spectra, and results of the two-pulse photon echo are reported for $Y_{2-x}Sc_xO_3$ ($x=0.04,0.3,1$) and YSZ (yttria-stabilized zirconia). For the $Y_{2-x}Sc_xO_3$ system, the inhomogeneous liinewidths increase with x while the homogeneous linewidths are nearly independent of x. Dynamics associated with low-frequency excitations observed previously in $x=0$ LHPG samples are nearly absent for $x>0$. However, both the static and dynamic properties of YSZ show behavior which is characteristic of amorphous systems like silicate glass.

I. INTRODUCTION

It is well known for amorphous materials that at low temperatures their dynamics is governed by the presence of two-level systems (TLS). In the optical domain, the existence of TLS is manifested by the appearance at low temperatures of a nearly linear dependence of the homogeneous linewidth on temperature ($\Gamma_H \propto T^n$ where n is slightly greater than or equal to 1). It has recently been shown for inorganic glasses[1] that the same value of n that is observed in the hole-burning results is also found for the temperature dependence of the specific heat, consistent with theoretical models.

It has also been reported that a number of disordered crystalline systems show a similar temperature dependence for the homogeneous linewidth. In optical hole-burning experiments of Sm^{2+} ions in the mixed crystalline system $BaFCl_{0.5}Br_{0.5}$ a temperature dependence with $n=1.27$ was observed for temperatures below 20 K.[2] Similarly, hole-burning experiments in the system yttria-stabilized zirconia (YSZ) doped with Pr^{3+} showed a similar behavior with $n=1.2$.[3] A linear term in the specific heat has also been observed in YSZ.[4] A variety of experiments also indicate the presence of TLS types of excitations in mixed crystals of the fluorite system. These include specific-heat experiments in $Ba_{1-x}La_xF_{2+x}$ (Ref. 5) and far-infrared absorption measurements in the same system or where the Ba is replaced by Ca.[6]

We recently reported[7] that the homogeneous linewidth of Eu^{3+} ions in the Y_2O_3 host grown by LHPG (laser-heated pedestal growth) and in one crystal grown by an arc image technique can be up to two orders of magnitude larger than that previously reported in a flame-fusion-grown crystal at 1.4 K, but that Γ_H in these samples is uncorrelated with their europium dopant concentration. We also found that the temperature dependence of Γ_H is nearly linear at low temperature (1.5–12 K) in contrast to the T^7 Raman behavior previously reported for good flame-fusion samples. While the temperature dependence of Γ_H was nearly the same as that found in amorphous systems, the magnitude of this nearly linear contribution to Γ_H is two or three orders less than that observed in glasses. A similar behavior has also been observed for Pr^{3+} ions in samples of Y_2O_3 grown by arc imaging under different atmospheres.[3]

In order to understand the role and mechanisms of disorder in determining Γ_H and its temperature dependence for crystalline materials, a study of the dynamical properties under systematic control of the disorder has been carried out. We thus present measurements of Γ_H and its temperature dependence for Eu^{3+} in a variety of mixed crystals with different levels of disorder. These include $Y_{2-x}Sc_xO_3$ ($x=0.04,0.3,1$) and yttria-stabilized zirconia (YSZ). We utilize the $^5D_0 \rightarrow {}^7F_0$ transition of Eu^{3+} ions. Four mixed crystals and a YSZ sample are examined using the two-pulse photon echo (TPPE) and spectral hole burning (SHB). These results are compared with those of Eu^{3+} ions doped in pure Y_2O_3 crystals and are correlated with the inhomogeneous linewidths of these same crystals. All samples used in these experiments have been grown by LHPG and all data shown here were measured at 1.5 K, except for the temperature dependence of Γ_H.

II. SPECTROSCOPY OF $Y_{2-x}Sc_xO_3$ ($x=0.04,0.3,1$) AND YSZ FIBERS

Both Y_2O_3 and Sc_2O_3 have the cubic (bixbyite) structure, whose lattice constants are $a_0=10.604$ and 9.845 A, respectively.[8] Its structure contains two inequivalent cation sites of C_2 and C_{3i} symmetry whose ratio is 3 to 1. Y_2O_3 and Sc_2O_3 form solid solutions over the full concentration range. Although it has been reported that the $x=1$ mixture, $YScO_3$, has an orthorhombic structure whose lattice constants are $a_0=5.43$ A, $b_0=5.712$ A, and $c_0=7.894$ A,[9] we believe that our LHPG sample probably had the cubic Y_2O_3 structure. The Eu^{3+} emission spectrum changed continuously within the series from Y_2O_3 to $YScO_3$ and $YScO_3$ behaved isotropically under a polarizing microscope.

Tissue *et al.*[10] reported that addition of Sc^{3+} ions to Er^{3+} doped in Y_2O_3 shifted the energy level positions, changed the inhomogeneous broadening and also shortened the fluorescence lifetime for Er^{3+} in the C_2 site.

Likewise, we find that the inhomogeneous absorption linewidths in $Y_{2-x}Sc_xO_3$:Eu^{3+} ($x=0.04,0.3$) were larger than those in Y_2O_3:Eu^{3+}, presumably due to random substitutional disorder in the mixed system. The $YScO_3$ ($x=1$) sample had a very broad inhomogeneous linewidth close to that of the highly disordered YSZ crystal.

YSZ, $(ZrO_2)_{1-y}(Y_2O_3)_y$, is stabilized in the cubic phase for $y=0.1$ to 0.7 at room temperature.[11] X-ray-diffraction measurements show that it has the fluorite structure with a lattice constant of $a_0=5.145$ A.[12] YSZ has a high ionic conductivity of oxygen ions that occurs primarily via the oxygen vacancies caused by the random substitution of Y^{3+} ions on the Zr^{4+} sites[4] where oxygen vacancies provide the charge compensation. Diffuse neutron-scattering measurements indicate random displacements of oxygen ions.[13] Such a random distribution of oxygens will act as a random potential on optical centers replacing Y^{3+} sites. YSZ thus has a significant disorder which is expected to lie midway between that of the crystalline and amorphous states.[9] Inhomogeneous broadening due to the random distribution of oxygen vacancies in YSZ was previously reported for Pr^{3+} ions.[3] Because of the disorder, the point group of trivalent rare-earth ions replacing yttrium in YSZ will have a symmetry lower than cubic.

The luminescence spectra of Eu^{3+} under excitation at 514.5 nm by an argon ion laser, in the region near the $^7F_0 \rightarrow {}^5D_0$ transition, are shown for a series of samples of $Y_{2-x}Sc_xO_3$ and of YSZ in Fig. 1. It illustrates the changes in transition energies and inhomogeneous linewidths for the Eu^{3+} transitions as the crystalline disorder is introduced. The luminescence spectrum of the 2% Sc mixed crystal ($x=0.04$) is similar to that of the flame-fusion bulk sample (not shown in Fig. 1), although some transitions are not well resolved in the 2% Sc mixed crystal due to the somewhat larger inhomogeneous linewidths. However, even with the larger inhomogeneous linewidths it is clearly seen that the $^5D_0 \rightarrow {}^7F_0$ transition, which occurs at 5808 A for $x=0$ samples shifts toward higher energies as the Sc^{3+} concentration is increased. The $^5D_0 \rightarrow {}^7F_0$ transition energy of Eu^{3+} ions in YSZ is larger than that of any of the $Y_{2-x}Sc_xO_3$ mixed crystalline samples and is shifted by 49 cm^{-1} relative to pure Y_2O_3.

The inhomogeneous linewidths increase rapidly with Sc^{3+} concentration, as was previously found for Er^{3+} ions.[10] Figure 2 summarizes the results on the inhomogeneous linewidths of the samples. We have previously shown that the inhomogeneous linewidth in pure Y_2O_3:Eu^{3+} (no Sc ions) single-crystal samples was characterized by a concentration-dependent broadening which increased from 5 to 25 GHz as the Eu^{3+} concentration was increased from 0.004 to 0.55 %, as would normally be expected for rare-earth-doped insulators. This is also summarized in Fig. 2. The addition of Sc ions produced an additional increase in the inhomogeneous linewidth. The inhomogeneous linewidth of the

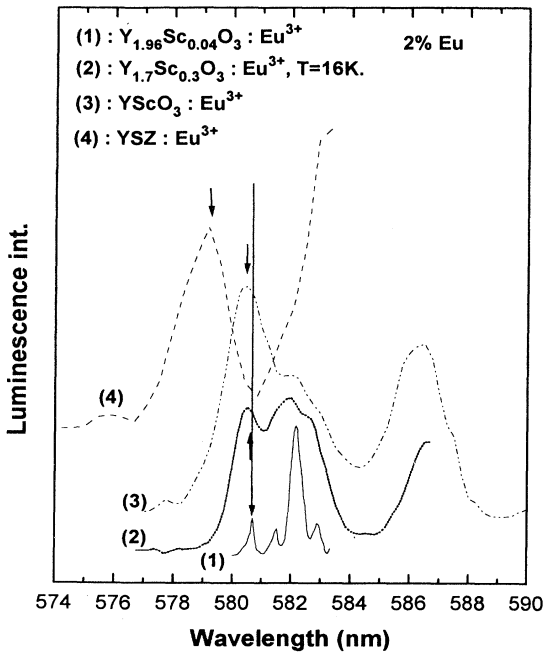

FIG. 1. Luminescence spectra near the $^5D_0 \rightarrow {}^7F_0$ transition for $Y_{2-x}Sc_xO_3$ ($x=0.04$, 0.3, 1) and YSZ fibers grown by LHPG at $T=1.5$ K. Excitation is made at 514.5 nm with an argon-ion laser so that both the Eu^{3+} (C_2) and Eu^{3+} (C_{3i}) sites are simultaneously excited. The arrows mark the $^5D_0 \rightarrow {}^7F_0$ transition where hole-burning was performed.

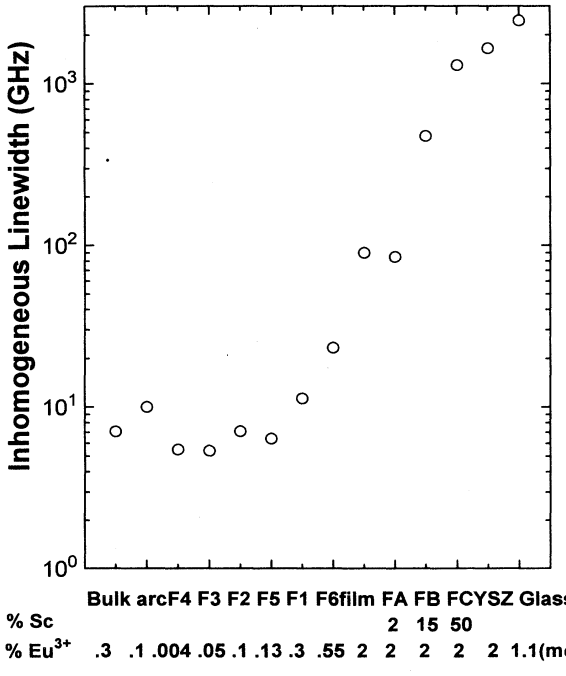

FIG. 2. Inhomogeneous linewidths of the $^7F_0 \rightarrow {}^5D_0$ transition in several Y_2O_3, $Y_{2-x}Sc_xO_3$ ($x=0.04$, 0.3, 1) and YSZ fibers, a thin Y_2O_3 film, and a silicate glass (Ref. 1). Measurements were all made at $T=1.5$ K (except for the glass where $T=77$ K). The inhomogeneous linewidths increase with dopant ion concentration due to random substitution of the impurity on the Y^{3+} site.

$^5D_0 \rightarrow {}^7F_0$ transition of Eu^{3+} ions reaches a maximum value of about 40 cm^{-1} in $YScO_3$ ($x=1$) which is almost as large as that found for the YSZ host crystal where it is 55 cm^{-1}. This is quite comparable with the linewidth found for this transition in silicate glass (also shown in Fig. 2), but much broader (25 times) than in pure single crystals of Y_2O_3:Eu^{3+} (2% Eu). The inhomogeneous linewidths of Eu^{3+} ions in $YScO_3$ and YSZ host materials thus lie intermediate between those of the good single crystal and those of an amorphous material such as a glass.

III. EXPERIMENT

TPPE and SHB experiments have been done in four mixed-crystal fibers (0.2% Eu^{3+}, 2% Sc, and 2% Eu^{3+}, $Y_{2-x}Sc_xO_3$; $x=0.04$, 0.3, and 1) and a YSZ crystal of composition $(ZrO_2)_{0.905}(Y_2O_3)_{0.095}$.

The fibers were grown by a laser-heated pedestal growth (LHPG) technique,[14] one of a number of methods available for the rapid preparation of crystalline materials. A sintered preparation material was melted at its upper end at the focus of a CO_2 laser. A seed crystal was then dipped into the melt, and a fiber of the material was drawn at a rate of about 1 mm/min. The resulting fibers were ~ 400 μm in diameter and some millimeters in length. The ends of each of the fibers were then polished, and a focused laser beam was observed to pass relatively unheeded through its length.

The fibers were all mounted on the same sample holder and placed in a helium immersion cryostat equipped with optical windows. For experiments at 1.4 K, the sample chamber could be filled with liquid helium from the reservoir, and the helium pumped below the λ point. For experiments above 2.1 K, a small heating element allowed a trickle of helium liquid from the reservoir to be warmed before it passed to the samples. The temperature could be varied from 2 to 14 K, with a stability of 0.2 K, and an accuracy ranging from 0.1 K at 4.5 K, to 1 K at 14 K.

The TPPE experiments were accomplished using a Coherent 599-21 single-frequency dye laser (bandwidth $\sim 2-3$ MHz), operating with Rhodamine R6G on the Eu^{3+} $^7F_0 \rightarrow {}^5D_0$ absorption. The laser beam was optically gated using two acousto-optic modulators (AOM) operating in tandom; two were used to ensure sufficient rejection of the laser radiation during the off period (rejection 10^{-5}). Two optical pulses were adjusted with respect to their pulse heights, widths, and the delay between the pulses. Optical pulse durations for the experiments were typically 600 ns ("$\pi/2$" pulse) and 850 ns ("π" pulse), and were directed into the cryostat windows through a 30 cm focal length lens (spot size at the crystals was ~ 50 μm). The laser power (cw) at the windows was ~ 10 mW. A good and reproducible launch into the fibers, without incurring any internal reflections, could be made by looking for a clear transmitted beam spot on the detection side of the cryostat. A particular path could be identified by collimating the output light with a second lens, and observing the spots as the beam was translated across the entrance face of the fiber. Passage of the laser beam off-axis through the fiber could clearly be seen as distortion of the output spot. The echoes were detected using a photomultiplier (EMI 9558) and Biomation (Model 6500), six-bit, 100 MHz, transient digitizer. Since the two preparation pulses and the echo were obtained with a collinear geometry, a double Pockels cell arrangement, each between crossed polarizers, was used to temporally protect the photomultiplier from the transmitted preparation pulses (transmission $<10^{-5}$) by gating the cells on after the second preparation pulse. The photon echo at each pulse separation was averaged for 100 to 2000 pulse pairs (repetition rate 10 Hz), and the data recorded on a computer.

Care was taken to avoid problems associated with hole burning of the Eu^{3+} transition, since the lifetime of the holes at liquid-helium temperatures may amount to several days.[15] During alignment of the laser beam through the fiber, and the positioning of the detection optics, the pulse repetition rate was increased to 100 kHz in order to view the transmitted beam. To avoid hole burning, this step in the experiment was made with the laser detuned from the transition, and it was only returned to line center when the repetition rate had been reduced to 10 Hz. Furthermore, all the echo decay measurements and optics alignment tasks were made with the laser scanning over about a 0.6 GHz range at approximately a 1 Hz repetition rate.

Hole-burning experiments were carried out by burning holes in the $^5D_0 \rightarrow {}^7F_0$ absorption band of Eu^{3+} ions by irradiating with the single-frequency dye laser. The laser light was passed through the two AOM's in tandem and then focused with a 3 in. focal lens on the sample. The holes were detected by measuring the emission or transmission spectrum depending on the absorption strength of the sample. For samples with a very weak absorption [$Y_{2-x}Sc_xO_3$ for $x=1$ and YSZ:Eu^{3+}(2%)], the holes were detected by a reduction in emission as the laser was scanned through the holes, while the holes in the more highly absorbing samples were detected by measuring the increased transmission. Measurements of the hole spectra were performed repetitively using a burn/delay/sweep/delay cycle and the averaged hole signal was recorded on a computer. The burn and sweep was performed with the laser attenuated with optical density filters (OD = 2.0–2.6), yielding a laser intensity of about 0.5 W/cm^2 on the sample. Following each individual recording of the hole spectrum, the laser was repetitively scanned about 10 or 15 times at full intensity (100 W/cm^2) so as to erase the hole. Burn times were of the order of 3 s, and the laser sweep rate was 2.4 MHz/ms for obtaining the total hole spectra and 0.4 MHz/ms for measuring the hole linewidth. Because of systematic variations of laser power during the scan, the background signal was subtracted from the hole spectra signals in order to obtain the hole spectra. The background signal was measured by setting the burn times to zero in the above burn/delay/sweep delay cycle. All hole spectra are shown with this background subtracted. Holes measured in transmission were burned with a small power and short time in order to avoid power-dependent effects such as power broadening and were averaged for 30–50 shots. All hole-burning experiments were done at $T=1.5$ K

and in the residual magnetic field ($\sim$200 G) of an electromagnet.

IV. RESULTS

The TPPE intensity for $Y_{2-x}Sc_xO_3:Eu^{3+}$ was measured as a function of the pulse separation τ. The data were fit to the expression

$$I=I_0\exp(-4\tau/T_2),$$

where I_0 is the echo intensity for $\tau=0$ and T_2 is the dephasing time. All echo decays were exponential except for the $x=0.3$ sample where a modulation in the echo decay was observed.

Photon echo decay curves for the mixed fibers are shown in Figs. 3 and 4. Figure 3 shows that there is a spatial dependence of the dephasing time in the $x=0.04$, 0.2% Eu^{3+} fiber as previously observed in the pure ($x=0$) Y_2O_3 fibers grown by the same LHPG method.[6] The two decay curves correspond to two different optical paths through the fiber and the dephasing is different almost by a factor 2 ($T_2=24.5$ μs and $T_2=47.7$ μs). Figure 4 shows that the echo decay for the $x=0.3$, 2% Eu^{3+} fiber was sharply rephased at $\tau=60$ μs. This rephasing is independent of magnetic field intensity up to 8.6 kG.

The magnitude of the homogeneous linewidths for Eu^{3+} ions in the pure[7] and mixed host materials is shown in Fig. 5. The homogeneous linewidths for the mixed crystal samples ($x=0.04$ and 1) were similar to that of the flame-fusion crystal. They were narrower by a factor of up to 8 times than that of Eu^{3+} ions in the pure Y_2O_3 fibers grown by the same LHPG technique and were unrelated to the inhomogeneous linewidth for each sample. The value of T_2 in the $x=0.3$ sample is difficult to determine because of the rephasing, but it is estimated as $T_2\cong 60$ μs. In general, the optical dephasing time does not depend strongly on either the Eu^{3+} or Sc^{3+} concentrations. However, T_2 for YSZ (2% Eu) at 1.5 K, was up to four orders of magnitude shorter than that of Eu^{3+} ions in the mixed fiber samples ($x=0.04$ and 1) or in the pure Y_2O_3 fibers.

It is surprising that fiber FC ($x=1$, 2 % Eu^{3+}) showed the longest T_2. This is in sharp contrast with the

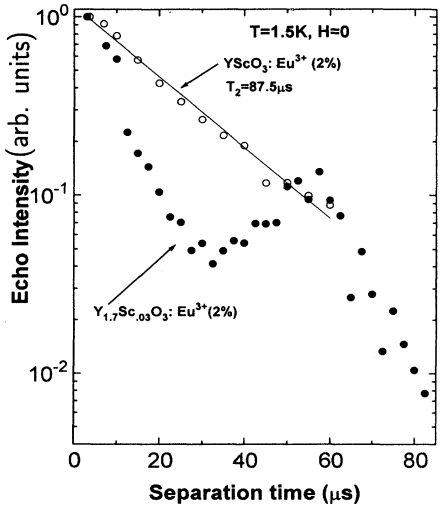

FIG. 4. Echo decay curves for fibers $Y_{1.7}Sc_{0.3}O_3$ (2% Eu) and $YScO_3$ (2% Eu). The echo decay in $YScO_3$ (2% Eu) shows an exponential decay and its dephasing time ($T_2=87.5$ μs) is comparable to that of the flame fusion crystal, in spite of its very broad inhomogeneous linewidth ($\sim$1300 GHz). In the $Y_{1.7}Sc_{0.3}O_3$ (2% Eu) fiber, a sharp rephasing was observed at $\tau=60$ μs.

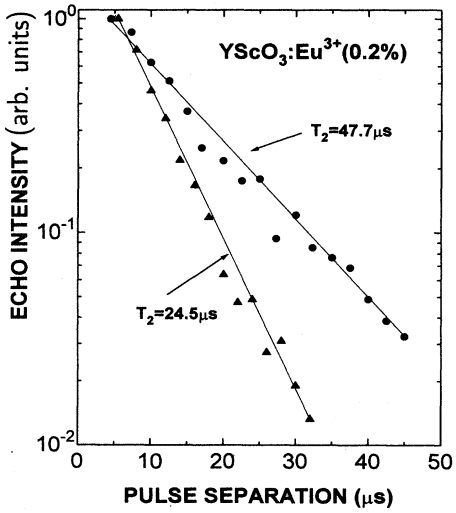

FIG. 3. Spatial dependence of the dephasing time. Two different echo decay curves were measured at the same temperature for a single $Y_{1.96}Sc_{0.04}O_3$ (0.2% Eu) fiber grown LHPG. The two decays correspond to two different topical paths through the fiber.

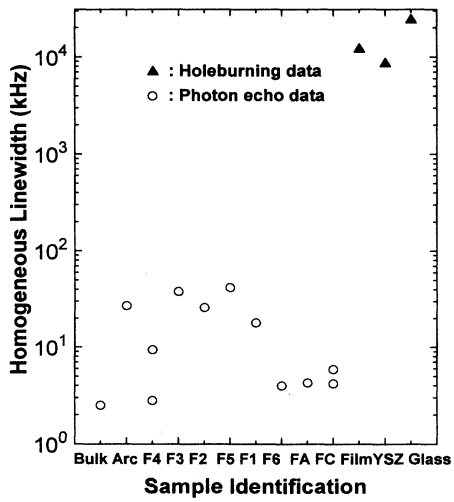

FIG. 5. Homogeneous linewidths for the same samples as in Fig. 2 measured by TPPE and SHB. The homogeneous linewidths in the FA ($Y_{1.96}Sc_{0.04}O_3:Eu^{3+}$, 2% Eu) and FC ($YScO_3:Eu^{3+}$, 2% Eu) fibers are narrower than that in pure Y_2O_3 fibers. Γ_H does not scale with Γ_{INH} in these samples.

behavior of the inhomogeneous linewidths which increase monotonically with Sc^{3+} concentration.

Figure 6 shows the temperature dependence of the optical dephasing rate T_2^{-1} for the fiber FC ($x=1$) which is nearly temperature independent until the onset of the two phonon Raman process at about 7 K as was found in the pure Y_2O_3 flame-fusion sample.[7] However, the inhomogeneous linewidth (1300 GHz) of this sample was closer to that of the highly disordered YSZ (1650 GHz) than it was to that of the pure Y_2O_3 flame-fusion sample (7.1 GHz).

Hole-burning spectra are shown in Fig. 7 for the flame-fusion and LHPG samples. The holes were long lived (10 min even in YSZ) and could be obtained up to 20 K. The anitholes due to the enhancement of the population in the nuclear quadruple levels of ^{151}Eu and ^{153}Eu (both $I=\frac{5}{2}$) are expected in Eu^{3+} at 1.5 K because the quadrupole splittings are larger than the homogeneous linewidth. Holes and antiholes were observed in the flame fusion bulk and $x=0.04$ crystals but the side holes were not clearly recognizable in the YSZ:2% Eu^{3+} sample.

The temperature dependence of the homogeneous linewidth determined from the hole spectrum in YSZ:Eu^{3+} is shown in Fig. 8. An instrumental contribution of 2 MHz has been subtracted from the measured data. Unlike the mixed-crystal system $Y_{2-x}Sc_xO_3$:Eu^{3+}, YSZ:Eu^{3+} shows a temperature dependence to the homogeneous linewidth. The temperature dependence can be fit with an expression

$$\Gamma_H(\mathrm{MHz})=9.5+0.48T$$

which consists of constant low-temperature term and a term proportional to T.

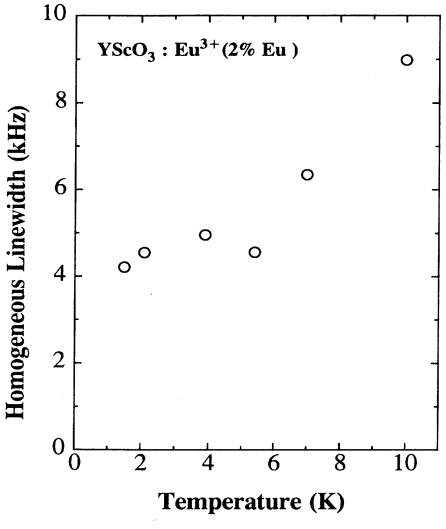

FIG. 6. Temperature dependence of homogeneous linewidth in the $YScO_3$ (2% Eu) fiber. Although the inhomogeneous linewidth suggests a highly disordered lattice, Γ_H is independent of T below 7 K and is consistent with a two-phonon Raman dephasing process at higher temperatures.

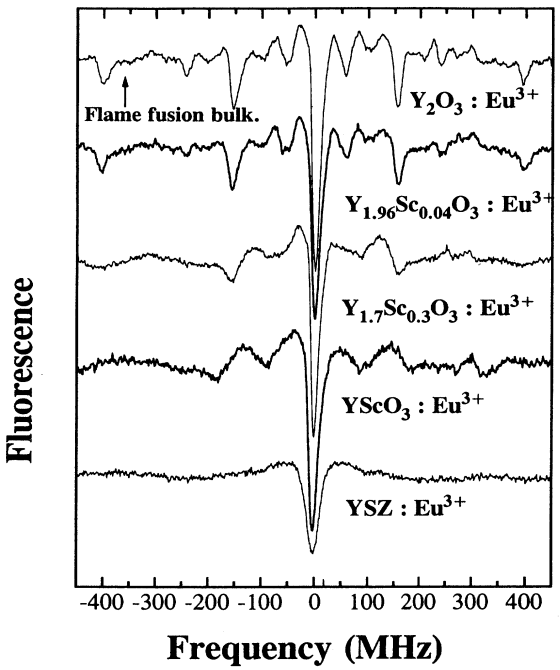

FIG. 7. Hole-burning spectra for some of the same samples as in Figs. 2 and 5. The central hole, side holes and antiholes are clearly recognizable in the Y_2O_3 flame-fusion bulk crystal and $Y_{1.96}Sc_{0.04}O_3$ (2% Eu) fiber. However, it is difficult to distinguish the side holes in the more disordered samples.

V. DISCUSSIONS

A. Homogeneous linewidth

1. $Y_{2-x}Sc_xO_3$:Eu^{3+}

Due to the extreme energy isolation of the ground- and excited-state levels, at low temperatures phonon-induced

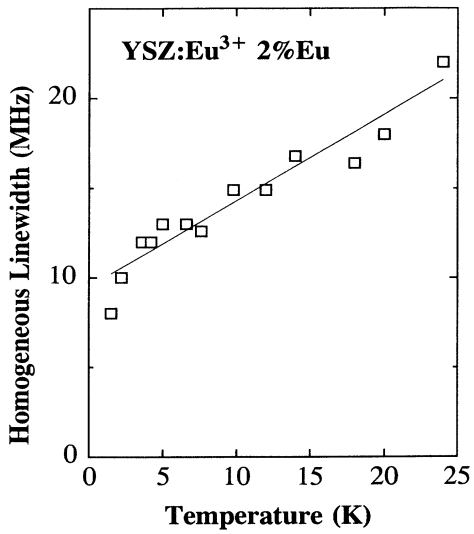

FIG. 8. Temperature dependence of the homogeneous linewidth in YSZ:Eu^{3+} from SHB experiments. Note the nearly linear temperature dependence between 2 and 20 K.

contributions to the homogeneous linewidth may be ignored. Therefore, at low temperatures and in well-ordered crystals with low dopant concentrations, the optical dephasing of optical transitions of Eu^{3+}, a non-Kramers rare-earth ion, is limited by interactions between the rare-earth magnetic moment and the fluctuating local fields due to surrounding nuclear spins.[16] Y_2O_3:Eu^{3+} is a typical example and its dephasing mechanisms have been discussed in the literature.[17]

In Y_2O_3:Eu^{3+}, only ^{89}Y has a nuclear magnetic moment among the host lattice ions and its magnitude is very small (-0.14_N). The magnitude of the local field due to ^{89}Y is expected to be only about 0.3 G. In addition, the nuclear spin flip rate, dominated by mutual spin flips of pairs of nuclei, should be very slow. This contribution to the homogeneous linewidth is therefore expected to be small (200–300 Hz).[17] No temperature dependence from this process is predicted, and indeed a high-quality, low Eu^{3+} concentration flame-fusion sample shows a temperature-independent dephasing below 8 K.[7]

However, the optical dephasing rates of all but one of the fibers of Eu^{3+} in Y_2O_3 grown by LHPG are much greater than that of the flame-fusion sample and below ≈ 8 K, the onset of significant contributions from the two-phonon Raman process, the homogeneous linewidths in the $x=0$ (pure) Y_2O_3:Eu^{3+} fibers show a nearly linear temperature dependence.[7] Magnetic interactions cannot account for the optical dephasing of Eu^{3+} ions in pure Y_2O_3 fibers grown by LHPG. The linear temperature dependence is characteristic of glasses or disordered crystalline systems[18,19] and therefore we suggested that highly local disorder, accompanied by a broad distribution of low-energy excitations, was responsible for this anomalous optical dephasing.[7]

In contrast to our expectation, the homogeneous linewidths of Eu^{3+} ions in disordered mixed samples, $Y_{2-x}Sc_xO_3$ ($x=0.04$, 0.3, 1) grown by LHPG were closer to that of the flame-fusion crystals than they were to the $x=0$ (pure) Y_2O_3:Eu^{3+} fibers and their homogeneous linewidths were not correlated with their inhomogeneous linewidths. The mixed crystal samples studied in this work differ in two ways from the $x=0$ Y_2O_3:Eu^{3+} samples described previously. They contain Sc^{3+} to produce cation site disorder and most of these samples contain 2% Eu^{3+}, a considerably higher concentration than that used in the pure Y_2O_3:Eu^{3+} studies.

In these 2% Eu^{3+} samples one must therefore consider Eu^{3+}-Eu^{3+} interactions. Huang *et al.*[20] determined that the homogeneous linewidth of 2% Eu^{3+} in Y_2O_3 (760 Hz) was due to Eu^{3+}-Eu^{3+} interactions (instantaneous diffusion). Instantaneous diffusion was identified by an increase in the homogeneous linewidth with an increase in the number of ions excited. In this case, Γ_H measured in a TPPE experiment increases with the energy in the echo preparation pulses. In addition, the homogeneous linewidth is expected to increase as the laser is tuned to the center of the absorption line where more ions are excited. We therefore would expect instantaneous diffusion to be greater in the $x=0.04$ sample than in the $x=1$ sample since the absorption coefficient of this sample is about 130 times greater than for the $x=1$ sample due to the fact that its linewidth is 130 times smaller producing a concomitant increase in the excited ion density. However, the measured homogeneous linewidths in these two samples are very similar to one another suggesting that instantaneous diffusion due to Eu^{3+}-Eu^{3+} interactions is not the dominant dephasing mechanism.

The addition of Sc^{3+} introduces a new large nuclear moment whose spin flips can produce additional dephasing. Its presence may also affect the occurrence of low-energy excitations which produce the anomalous dephasing in pure Y_2O_3:Eu^{3+} samples. The nuclear magnetic moment of ^{45}Sc ($I=+4.7564$) is comparable to that of ^{27}Al ($I=+3.6414$). Shelby and Macfarlane[21] confirmed that dephasing in $YAlO_3$:Eu^{3+} is due to the fluctuating field from ^{27}Al nuclei interacting with ^{151}Eu and ^{153}Eu nuclear magnetic moments. Since the ground-state nuclear moments of Eu^{3+} ions are anomalously small,[19] most of the width results from excited-state interactions. For the $x=1$ sample, it is therefore expected that the dephasing in $YScO_3$:Eu^{3+}, due to ^{45}Sc nuclear spin dynamics, would be similar to the dephasing in $YAlO_3$:Eu^{3+}. The observed homogeneous linewidth of Eu^{3+} in $YScO_3$:Eu^{3+} (3.6–5.9 kHz) is indeed comparable to that found in $YAlO_3$:Eu^{3+} (5.5 kHz). We therefore believe that the main dephasing mechanism in Eu^{3+} in $YScO_3$ LHPG fibers will be the interaction between the nuclear magnetic moments of ^{45}Sc and the nuclear magnetic moments of ^{151}Eu, ^{153}Eu. This is supported by the data in Fig. 9 which shows that the optical dephasing in $YScO_3$ depends on the magnetic field intensity. A similar decrease in Γ_H was found in $YAlO_3$:Eu^{3+} in the presence of a magnetic field (linewidth deceases from 5.5 to 3.1 kHz in a field of 375 G).[21]

However, nuclear spin dynamics are probably not the only source of dephasing. First of all, the $x=0.04$ sample has similar homogeneous linewidth to the $x=1$ sample even though the Sc^{3+} concentration is only 2%. We suggest that the dephasing consists of contributions from both nuclear spin flips and TLS-type of dynamics. Sc^{3+}

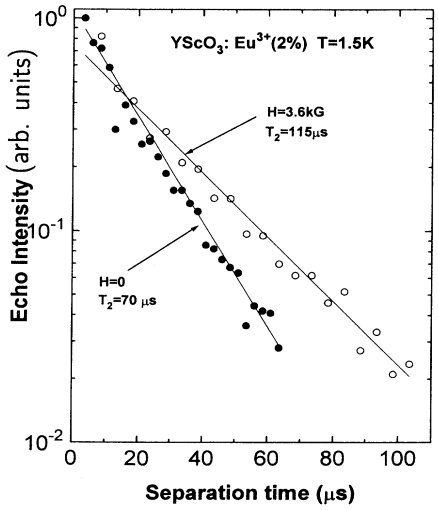

FIG. 9. Magnetic-field dependence of optical dephasing in the $YScO_3$ (2% Eu^{3+}) fiber. T_2 increases in a magnetic field.

may stabilize the oxygen stoichiometry, helping to eliminate the defects responsible for the TLS-type of low-frequency modes which contribute to the dynamics at low temperatures. As the Sc^{3+} concentration is raised, contributions to Γ_H from TLS are reduced while contributions from ^{45}Sc nuclear spin dynamics are increased; the two competing effects maintain a fairly constant value of Γ_H with an increase in x. The observation of a spatial dependence to Γ_H for the $x=0.04$ fiber, as previously seen in the $x=0$ LHPG fibers, indicates that TLS-type contributions to the dephasing are still present for the $x=0.04$ sample. In contrast, we surmise that in the $x=1$ sample the TLS-type of contributions have become less important, reduced by the high concentration of Sc^{3+}, while the nuclear spin dynamics due to the ^{45}Sc have become dominant.

2. *YSZ:Eu^{3+}*

The existence of a temperature dependence of the homogeneous linewidth at low temperatures in YSZ:Eu^{3+} points to the presence of a dynamical process associated with low-energy excitations like the TLS found in glasses. However, the temperature dependence of YSZ:Eu^{3+} is different from that of Eu^{3+} in glasses[1] and Pr^{3+} in both YSZ (Ref. 3) and glasses,[1] as shown in Fig. 10, in that it does not extrapolate to zero at zero temperature (see also Fig. 8). Both Eu^{3+} and Pr^{3+} in silicate glass show a nearly linear temperature dependence to the homogeneous linewidth down to 0.4 K which contributes about 10 and 30 MHz, respectively, at 1 K. In contrast, for YSZ:Eu^{3+} the temperature-dependent contribution is an order of magnitude smaller and there is an additional contribution present at 1.4 K whose temperature dependence is unknown from these experiments which do not go below 1.4 K.

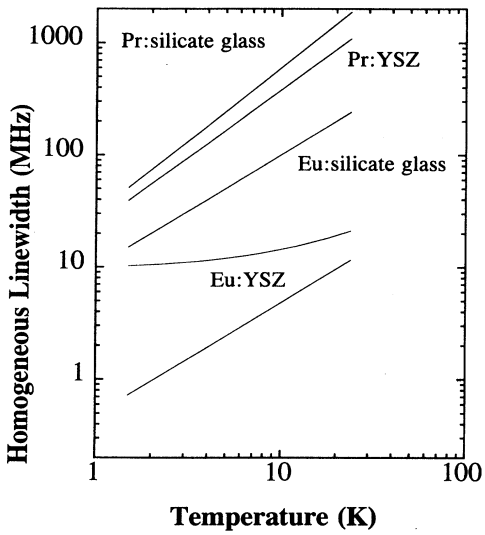

FIG. 10. Comparison of the temperature dependence of Γ_H for Eu^{3+}- and Pr^{3+}-doped silicate glasses (Ref. 1) and YSZ:Pr^{3+} (Ref. 3) with YSZ:Eu^{3+} (present study). The upper curve for YSZ:Eu^{3+} is the actual data while for the lower curve the constant low temperature ($T\rightarrow 0$) contribution has been subtracted to exhibit the linear temperature dependence.

It was observed[3] that the temperature-dependent linewidth for Pr^{3+} ions in YSZ was similar to that for Pr^{3+} ions in silicate glass ($\frac{1}{3}$ the value found in their silicate glass sample and nearly the same value as reported in Ref. 1). The temperature dependence observed for YSZ:Pr^{3+} was $\Gamma_H \propto T^{1.2}$. When the low-temperature extrapolated value of Γ_H for YSZ:Eu^{3+} (value at 1.4 K) is subtracted from the data at higher temperatures, it is clearly seen that the magnitude of the nearly linear temperature dependence of Γ_H (see Fig. 10, bottom curve) is much smaller than that of Pr^{3+} in either YSZ or silicate glass and a factor of 1/20 that found for Eu^{3+} in silicate glass. Thus, while the data point to the presence of low-lying excitations in YSZ:Eu^{3+}, the contribution is much smaller than that observed for Eu^{3+} in silicate glasses or for Pr^{3+} in either YSZ or silicate glass.

It should also be noted that the hole-burning results in YSZ may not truly describe the homogeneous linewidth. If spectral diffusion occurs in this system, the hole-burning results may contain a contribution from time-dependent broadening which will depend on the time scale of the experiments. This is well known in other disordered systems.[22] Clearly further studies of the homogeneous linewidth in YSZ are needed to fully resolve the role of TLS and the nature of the dynamics of this system.

B. Echo modulation of $Y_{0.3}Sc_{1.7}O_3$:Eu^{3+}

Finally we comment on the modulation which appears in the $x=0.3$ fiber. In this sample, we observed a sharp rephasing in the echo intensity decay curve at $\tau=60$ μs (see Fig. 4). Echo modulations usually arise from an interference among the energy states, referred to as quantum beat echo modulations.[23] For example, Chen, Chiang, and Hartman[24] reported a modulated photon echo for the $^3P_0\rightarrow{}^3H_4$ transition in LaF_3:Pr^{3+} (0.03%). They explained that this modulated photon echo was due to the nuclear quadrupole splitting of the $^3P_0$ and $^3H_4$ states. The echo modulation in $Y_{1.7}Sc_{0.3}O_3$:Eu^{3+} (2%) was independent of magnetic field (up to 8.5 kG) which is inconsistent with the above mechanism since the quadrupole levels would split in the field. However, the bandwidth of the laser used in the present experiments (2 MHz) is too narrow to prepare a superposition of hyperfine levels which are separated by ≈ 100 MHz. Instead, the modulations may be connected with the Eu^{3+}-Sc^{3+} superhyperfine interactions since for $x=0.3$ each Eu^{3+} has about one nearest-neighbor Sc^{3+}. The ^{45}Sc-^{151}Eu superhyperfine interaction for nearest-neighbor nuclei is $\mu_{Eu}\mu_{Sc}/r^3=8$ kHz, of the right order of magnitude to explain a 16 kHz modulation. However, for the $x=1$ sample, the hyperfine structure becomes quite complicated with many Sc nearest-neighbor nuclei, thereby washing out the modulation patterns.

C. Hole structure and lifetime

Figure 7 shows that the central hole and antiholes are clearly recognizable in all samples, but that there are no

distinct side holes in the highly disordered systems [YSZ, $YScO_3$ ($x=1$)]. The hole spectra in the flame-fusion (bulk) and 2% Eu^{3+}, $x=0.04$ fiber are quite similar to each other. However, as the inhomogeneous linewidth increases, it becomes difficult to distinguish the side holes. As x increases in the system $Y_{2-x}Sc_xO_3$:Eu^{3+}, the side-hole splittings seem to become larger indicating an increase in the quadrupole splittings with increased Sc^{3+} concentration. The antihole structure in YSZ is very similar to that observed for Eu^{3+} in silicate glass. The fact that there are no side holes in YSZ and glass probably results from the broadening of the distribution of the ground- and/or excited-state quadrupole splittings. The observed hole widths in these spectra are limited by a combination of the laser bandwidth (2–3 MHz) which contributes up to 6 MHz and the rapid scan rate (2.4 MHz/ms) which because of the fluorescence detection and 1 ms excited-state lifetime, contributes ~5 MHz. As a result, these spectra cannot be used to obtain the hole widths.

The hole lifetime was long (10 min even in YSZ) at 1.5 K and could be obtained up to 20 K. This is distinct from quadrupole level hole lifetimes of Eu^{3+} in glasses where it is typically about 10 s.[18] Evidently, the broadening of the hole structure in YSZ is not as great or it has a different spectral distribution than that in silicate glass so that the broadening is not as efficient in YSZ relative to the glass in allowing spin-lattice relaxation among the quadrupole levels.

Macfarlane and Shelby reported two types of mechanisms for producing long-lived holes in glasses.[18] One is an optical pumping mechanism of the nuclear quadrupole levels which is observed for the $^7F_0 \rightarrow {}^5D_0$ transition of Eu^{3+} ions in silicate glass. The other is a photophysical process which involves an optically induced rearrangement of the local environment of the irradiated ions which was observed for Pr^{3+} in silicate glass.[1] This can be described in terms of TLS. As for Eu^{3+} in glass[1] only the quadrupole level storage has been observed in YSZ and $Y_{2-x}Sc_xO_3$:Eu^{3+}.

VI. CONCLUSIONS

The homogeneous and inhomogeneous linewidths of Eu^{3+} in disordered systems, where the disorder is produced in a controlled manner, have been examined. For $Y_{2-x}Sc_xO_3$ grown by LHPG the inhomogeneous linewidths increase continuously as the disorder is increased (increase in x), going from 0.4 cm^{-1} for $x=0$ to 40 cm^{-1} at $x=1$. A broadening of the quadrupole splittings is also observed in the hole-burning spectra. In contrast, the homogeneous linewidth is nearly independent of x and is actually larger for the $x=0$ LHPG samples, by up to a factor of 8, than for the samples with $x=0.04$, 0.3, and 1. In addition, while the $x=0$ fibers show a linear temperature dependence for Γ_H, the $x=1$ fiber shows a temperature independence for Γ_H below 7 K. We conclude that while the replacement of trivalent Y with trivalent Sc leads to an increase in the static disorder, this disorder does not lead to an increase in the dynamical properties of the $Y_{2-x}Sc_xO_3$ system. Rather, the introduction of Sc^{3+} seems to reduce the dynamics associated with the low-frequency excitation modes found in previous studies[7] for the $x=0$ (pure) LHPG samples containing Eu^{3+}.

In sharp contrast, for YSZ:Eu^{3+} (2%), where the substitution of *tetravalent* Zr by *trivalent* Y leads to oxygen vacancies because of the requirement for charge compensation, both the inhomogeneous and homogeneous linewidths of Eu^{3+} are dramatically increased relative to well-ordered crystalline systems. It thus appears that disorder on the oxygen sublattice may lead to the generation of the low-energy excitations responsible for the increased dynamical properties of YSZ, as manifested in its large homogeneous linewidth which contributes a linear temperature-dependent term to Γ_H.

The Y_2O_3 structure can be thought of as a distortion of the CaF_2 structure, where the metallic ions are distributed as the calcium ions but the oxygen ions occupy only three-fourths of the fluorine positions.[8] With one-fourth of the anion sites vacant, this structure seems susceptible for defects on the oxygen sublattice. These defects may be responsible for the dynamics of the $x=0$ (pure) samples seen in the previous studies.[7] Addition of Sc^{3+} seems to reduce the dephasing, perhaps by reducing the number of oxygen sublattice defects.

ACKNOWLEDGMENTS

We thank Lizhu Lu for growing the LHPG samples and Roger M. Macfarlane for helpful discussions. We acknowledge the support of the National Science Foundation, Grant No. DMR-9321052.

[1]Th. Schmidt, R. M. Macfarlane, and S. Volker, Phys. Rev. B **21**, 15 707 (1994).

[2]C. Wei, K. Holliday, A. J. Meixner, M. Croci, and U. P. Wild, J. Lumin. **50**, 89 (1991); K. Holliday, C. Wei, M. Croci, and U. P. Wild, *ibid.* **53**, 227 (1992).

[3]K. Tanaka, T. Okuno, H. Yugami, M. Ishiame, and T. Suemoto, Opt. Commun. **86**, 45 (1991); T. Okuno, K. Tanaka, K. Koyama, M. Namiki, and T. Suemoto, J. Lumin. **58**, 184 (1994).

[4]W. N. Lawless, Phys. Rev. B **22**, 3122 (1980).

[5]D. G. Cahill and R. O. Pohl, Phys. Rev. B **39**, 10 477 (1989).

[6]S. P. Love, C. E. Mungan, A. J. Sievers, and J. A. Campbell, J. Opt. Soc. Am. B **9**, 794 (1992).

[7]G. P. Flinn, K. W. Jang, Joseph Ganem, M. L. Jones, R. S. Meltzer, and R. M. Macfarlane, Phys. Rev. B **49**, 5821 (1994).

[8]Ralph W. G. Wyckoff, *Crystal Structure,* 2nd ed. (Interscience, New York, 1960), Vol. 2, p. 3.

[9]Ralph W. G. Wyckoff, *Crystal Structure* (Ref. 8), p. 407.

[10]B. M. Tissue, N. J. Cockroft, Lizhu Lu, D. C. Nguyen, and W. M. Yen, J. Lumin. **48/49**, 477 (1991).

[11]C. Puscal and P. Duran, J. Am. Ceram. Soc. **66**, 23 (1983).

[12]E. Greenberg, G. Katz, R. Reisfeld, N. Spector, R. C. Marshall, B. Bendow, and R. N. Brown, J. Chem. Phys. **77**, 4794 (1982).

[13]D. Steele and B. E. F. Fender, J. Phys. C **7**, 1 (1974).
[14]R. S. Fiegelson, J. Crsyt. Growth **79**, 669 (1986).
[15]W. R. Babbitt, A. Lezama, and T. W. Mossberg, Phys. Rev. B **39**, 1987 (1989).
[16]R. M. Macfarlane and R. M. Shelby, in *Spectroscopy of Solids Containing Rare Earth Ions,* edited by A. A. Kaplyanskii and R. M. Macfarlane (North-Holland, Amsterdam, 1987).
[17]R. M. Macfarlane and R. M. Shelby, Opt. Commun. **39**, 169 (1981).
[18]R. M. Macfarlane and R. M. Shelby, Opt. Commun. **45**, 46 (1983).
[19]R. M. Macfarlane and R. M. Shelby, J. Lumin. **36**, 179 (1987).
[20]Jin Huang, J. M. Zhang. A. Lezama, and T. W. Mossberg, Phys. Rev. Lett. **63**, 78 (1989).
[21]R. M. Shelby and R. M. Macfarlane, Phys. Rev. Lett. **45**, 1098 (1980).
[22]W. S. Brockelsby, B. Golding, and J. R. Simpson, J. Lumin. **45**, 54 (1990).
[23]R. M. Macfarlane and R. M. Shelby, in *Spectroscopy of Solids Containing Rare Earth Ions* (Ref. 16), p. 153.
[24]Y. C. Chen, K. Chiang, and S. R. Hartmann, Phys. Rev. B **21**, 21 (1980).